Version of Record: https://www.sciencedirect.com/science/article/pii/S0079610717300822
Manuscript_81e4a204b64cf1a4e8fdefcb13e445e8

On the effects of glasses on the SAR in human head resulting from wireless eyewear devices at phone call state

J. Q. Lan[a], X. Liang[a], T. Hong[b], G. H. Du[a, *]

[a]Chengdu University of Information Technology, Chengdu, 610225, China

[b]China West Normal University, Nanchong, 637002, China

Abstract:

This paper evaluates the effects of glasses on the specific absorption rates (SAR) in the human head resulting from wireless eyewear device at phone call state. We mainly concentrate on the SAR in the eyes since their sensitivity to electromagnetic fields (EMF). We find wearing glasses obviously alters the distribution and magnitude of the SAR. The maximal SAR in the ocular tissues with glasses is even 6 times more than that without glasses. Wearing glasses also induce the new hotspot in the eyes which may cause the biggest SAR increment in the ocular tissues. Moreover, calculated results indicate that the maximal SAR is sensitive to the size of glasses and radiation frequency. Because of this，we believe wearing glasses may possibly increase the risk of health hazard to eyes of wireless eyewear device user. These calculated results could be a valuable reference for the glasses designer to reduce the SAR in the eyes.

Keywords: SAR; wireless eyewear device; FDTD; eyes; Glasses; phone

1. Introduction

The widespread use of mobile phone has led to strong public concern whether it is harmful to human health. According to the research report from International Agency for Research on Cancer (IARC), radiation from mobile phone may possibly increase the risk of getting glioma and acoustic neuroma (IARC, 2011). For this reason, although safety standards such as IEEE C95.1:2005 (IEEE Standard for Safety, 2010) and ICNIRP (Ahlbom et al., 1998), have been established, they are not entirely reliable. SAR is

© 2018 published by Elsevier. This manuscript is made available under the Elsevier user license
https://www.elsevier.com/open-access/userlicense/1.0/

usually used to evaluate the interaction between EMF and biological tissue, which depends not only on the EMF including radiation frequency, field strength, polarization and etc, but also the geometry and material property of biological tissues. There are many valuable researches (Yoshida et al., 2005; Manapati and Kshetrimayum, 2009; Wake et al., 2009; Hossain et al., 2015; Anzaldi et al., 2007; Beard et al., 2006; Chandupatla et al., 2006; Pisa et al., 2005; Schiavoni et al., 2000; Van et al., 1999; Scott, 1988; Cabedo et al., 2009; Anguera et al., 2010; Picher et al., 2012; Lan and Huang, 2013; Whittow et al., 2008; Virtanen et al., 2007; Cihangir et al., 2014, Whittow W., 2004) which have evaluated the interaction between human body and EMF from mobile phone. Some of them have found the objects adjacent to the human head might greatly modify the nearby EMF from the mobile phone and pose a potential health hazards to human body. For example, Whittow et al evaluated the effects of the metallic jewelry on the SAR in the human head and found the SAR might be several times larger than that without wearing jewelry (Whittow et al., 2008). Virtanen found metallic implants could double the magnitude of SAR in the human head (Virtanen et al., 2007).

In recent years, there are increasing interests in wireless eyewear devices (EyeTrek Insight Smart glasses, Mad Gaze X5 and so on). Although these devices are just limited to wireless Bluetooth and Wi-Fi connection currently, there is clearly a need for connecting to the cellular network in the future (Cihangir et al., 2014; Cihangir et al., 2014). The wireless eyewear device is usually placed on the side of one eye by fixing on the glasses, metallic frame, eye patch, ear and so on. Among them, glasses are the main choice. This is due to the reason that myopia as a typical epidemic has higher morbidity rate around the world, especially in East Asian. There would be 2.5 billion people with myopia by the year 2020 (Brien et al., 2004). Therefore, maybe half of wireless eyewear device users would choose glasses.

In order to evaluate whether wearing glasses may lead to health risks to the wireless eyewear device user, this paper would evaluate the relative effects of metallic frame

glasses on the SAR in the human head at phone call state. We will mainly concentrate on the ocular tissues due to its sensitivity to EM fields (Dimbylow and Mann 1994; Dovrat et al., 2005). This is because eyes are directly exposed to the electromagnetic radiation without the protection of skin, fat and so on. what's more, eyes could not dissipate the heat induced by electromagnetic radiation timely because of the lower blood flow. Thirdly, once ocular tissues are damaged, they could not return to be healthy because ocular tissues except the cornea lack the self-renewal ability. A rigorous FDTD CAD model which include a three-dimensional (3D) anatomical human head model, a pair of glasses and a type of wireless eyewear device is established. The head model consists of skin, fat , brain and elaborate eyeballs which are made of eight kinds of tissues. A printed coupling element (CE) antenna is designed for eyewear device. It covers 0.75-0.93 and 1.63-1.86 GHz with a -6dB S_{11}. This paper would mainly focus on the relative effects of glasses on the SAR in the head of wireless eyewear device user compared to an absence of glasses applied to the exposure condition at phone call state. These calculated results may be a valuable reference for the glasses designer to reduce the SAR in the eyes.

2. Simulation models and materials

2.1. HEAD MODEL

The CAD model, compared with the traditional Magnetic Resonance Imaging (MRI) or Visible Human Project (VHP) models, could provide the higher resolution. Therefore, a three-dimensional (3D) anatomical human head CAD model shown in Fig.1 is established in this paper. This model chooses the average size of typical Chinese adult man, which includes skin, fat and elaborate eyeball. Fig.2 is the cross-section of eyeball. It shows the detailed structures of the human eyes. The eyeball is made of eight kinds of tissues. The resolution of 0.2 mm is proposed to accurately model the configuration of ocular tissues. Each tissue is represented by homogeneous isotropic medium. The dielectric properties and density of tissues are displayed in table 1 (Van et al., 1999; Dimbylow and Mann 1994; Rodrigues et al., 2008; Lin, 2005; Gandhi, 1996; Jensen and

Rahmat-Samii, 1995; Dimbylowt and Gandhif, 1991; Scott, 1988; Gabriel, 1983). ε_r and σ represent the relative dielectric constant and conductivity, respectively.

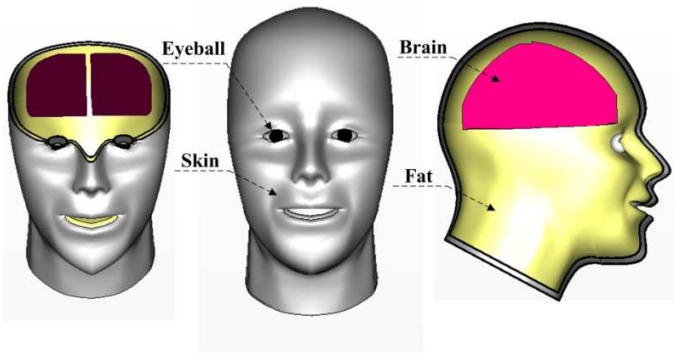

Fig. 1. Human head model.

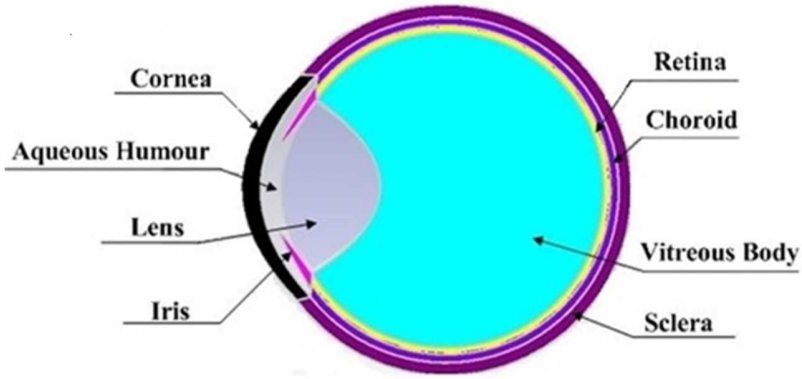

Fig. 2. Cross-section of eyeball.

Table 1

The dielectric properties and density of tissues in the human head model.

Biomaterial	0.915 (GHz)		1.8 (GHz)		Density(kg/m^3)
	ε_r	σ	ε_r	σ	
Cornea	51.5	1.9	73.9	2.21	1050

Iris	55	1.18	49.41	1.64	1040
Air	1	0	1	0	0.0016
Skin	45	0.97	37.21	1.25	1100
Choroid	55	2.3	76	2.88	1000
Lens	44	0.8	42.02	1.15	1150
Sclera	51	1.13	52.56	1.73	1020
Aqucous Humor	74	1.97	74	2.27	1010
Vitreous Body	67	1.68	73.9	2.21	1030
Retina	57	1.17	78.4	2.11	1000
Fat	15	0.35	9.38	0.26	920

2.2. GLASSES MODEL

The glasses used in this paper are shown in Fig. 3. Compared with the former study (Cihangir et al., 2014) that only evaluates the single metallic frame, this model consists of spectacle frame, spectacle lens and nose pad. W_1 and W_2 are the width of frame. The thickness of frame is 1 mm. W_3 represents the thickness of spectacle lens. W_4 is the length of glasses arm. The distance between two arms are 155mm. Glass (ε_r=4.82, σ=0.0054) and polyimide (ε_r=3.5, σ=0.03) are selected as the material of spectacle lens and nose pad, respectively. The Spectacle frames are usually made of plastic or metal. Plastic could be made into various of patterns, while it would lose its form with daily use. By contrast, metal frame has many advantages. For instance, Monel has well ductility which could be made into various of shapes without losing strength. Copper has good corrosion resistance. Metal material, therefore, is more suitable for eyewear device because the spectacle frame is also used to support the printed circuit board of the eyewear device. Furthermore, the author (Whittow, 2004) have proved that the variation in conductivity

posed negligible variation to the SAR in the human head. So this paper would use the copper frame.

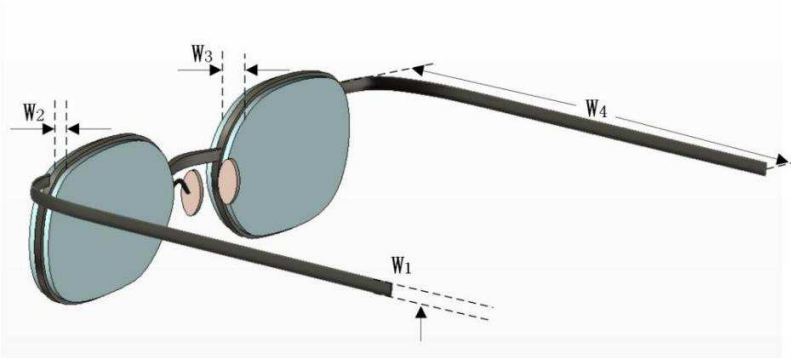

Fig. 3. Model of glasses.

2.3. ANTENNA MODEL

In this paper, we employ a kind of printed coupling element (CE) antennas designed for eyewear device (Cihangir et al., 2014; Cihangir et al., 2014). As is shown in Fig. 4, the ground plane is printed on the one side of the FR4 printed circuit board (PCB). The CE is on the other side of the PCB, which is adjacent to the eyes. The antenna is fed by a three-element matching network (MN) which includes of a shunt capacitor and two series inductors. By adjusting the MN, the antenna could be transformed into the desired operating band. Fig. 5 shows the calculated results of S_{11} of the antenna with head model at two frequencies shown in Fig. 6. It covers 0.75-0.93 and 1.63-1.86 GHz with a -6dB S_{11}. The input power of the antenna is 0.125W since a GSM terminal only transmits for one-eighth of the time.

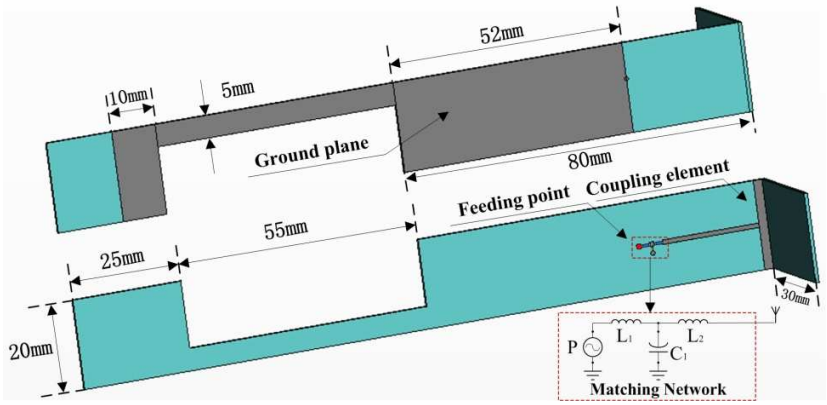

Fig. 4. Antenna model for eyewear device.

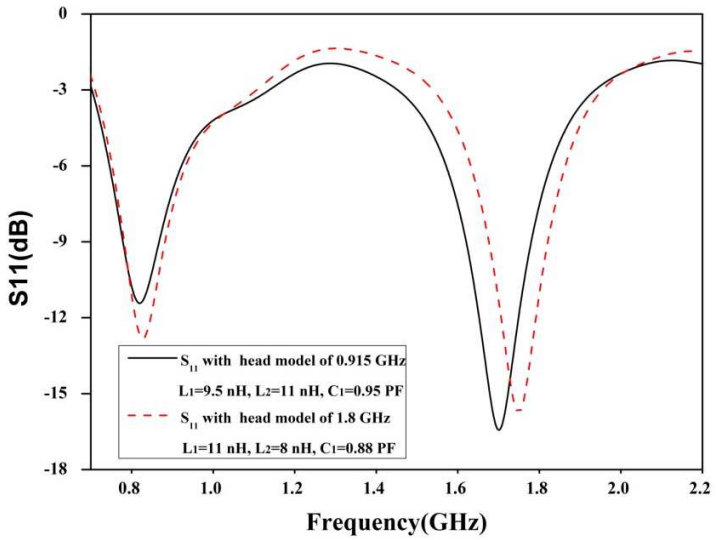

Fig. 5. S_{11} of the antenna with head model.

3. Calculation result and discussion

Based on the FDTD method (Yee, 1966; Sacks, et al., 1995; Gedney, 1996), the whole computational region is divided by regular hexahedron grids. The size of the background grid is 2 mm. We employ the sub-gridding method since the sophisticated eyeball structure which includes of multilayer ultra-thin millimeter-scale membrane structure (Kunz and Luebbers, 1993). The sub-grids of 0.2 and 0.5 mm is used to represent the

eyeball and other parts of the simulation model.

For ease of understanding, this paper introduces the sub-gridding method for the two-dimensional case of TE propagation mode . The discretized Maxwell's equations are as follows:

$$H_x^{n+1/2}\left(i,k+\frac{1}{2}\right) = H_x^{n-1/2}\left(i,k+\frac{1}{2}\right)+\frac{c\Delta t}{Z_0\Delta z}[E_y^{n}(i,k+1)-E_y^{n}(i,k)] \tag{1}$$

$$H_z^{n+1/2}\left(i+\frac{1}{2},k\right) = H_z^{n-1/2}\left(i+\frac{1}{2},k\right)-\frac{c\Delta t}{Z_0\Delta z}[E_y^{n}(i+1,k)-E_y^{n}(i,k)] \tag{2}$$

$$E_y^{n+1}(i,k) = E_y^{n}(i,k)+\frac{Z_0 c\Delta t}{\Delta z}[H_x^{n+1/2}\left(i,k+\frac{1}{2}\right)-H_x^{n+1/2}\left(i,k-\frac{1}{2}\right)] -\frac{Z_0 c\Delta t}{\Delta x}[H_z^{n+1/2}\left(i+\frac{1}{2},k\right)-H_z^{n+1/2}\left(i-\frac{1}{2},k\right)] \tag{3}$$

where i and k refer to the Cartesian coordinates x and z, respectively. The computational area for the TE propagation mode and field vector components are shown in Fig. 6. The detailed sub-gridding method is shown in (Kim and Hoefer, 1990). According to the sub-gridding method, the primary task of the sub-gridding method is to make sure that the fields across the interfaces between coarse and fine grids must be continuous. Furthermore, the local uniformity of the grids is crucial to keep the same stability criterion in the process of the calculation. Thirdly, in the case of a grids ratio shown in Fig. 6, the time increment in the coarse grids must be four times as large as that in the fine grids (Any integer grids ratio could be chosen). The uniaxial perfectly matched layer with 5 cells thick is used as the absorbing boundary to terminate the computational

domain. The relative accuracy is 10^{-5}. The sub-gridding method greatly increases computational cost, but it effectively ensures the accuracy of the calculated results. Because of the sensitivity of eyes to EMF, we focus on the SAR for 1 g in eyes upset by the glasses at phone call state shown in Fig. 7. To calculate SAR for 1 g, we add contributions of several Yee's meshes to 1 g around the cube of the maximum SAR. (In this paper, all SAR refers to the SAR for 1 g.)

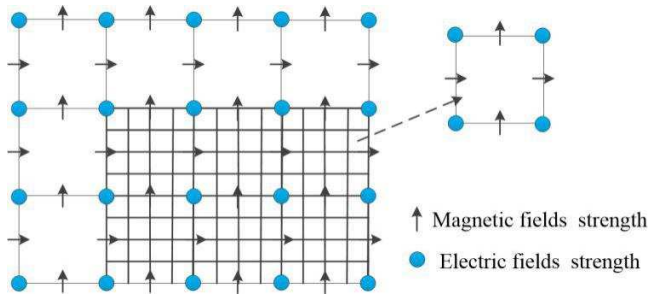

Fig. 6. the 1:4 sub-gridding method in two-dimensional local area.

We firstly calculate the SAR distribution in the human head when people do and don't wear glasses. Fig. 8 shows the SAR distribution in the human head. We can see that wearing glasses obviously alters the distribution and magnitude of SAR. The maximum SAR in the human head has increased about 2.5 times when people wear glasses. Fig. 9 and Fig. 10 show the SAR distribution in the eyeballs at 0.915GHz and 1.8 GHz. The maximum SAR in eyeballs with glass is almost three times more than that without glasses. Wearing glasses leads to the new hotspots in the eyeballs, which could be found by comparing the SAR in the two-dimensional (2D) cross-section of eyeball with and without glasses. We also show the maximal SAR of ocular tissues in Fig. 11. The maximal SAR has increased to 1.7 to 6 times when people wear glasses. Therefore, wearing glasses may possibly induce higher risk of the health hazard to eyes of the wireless eyewear device user.

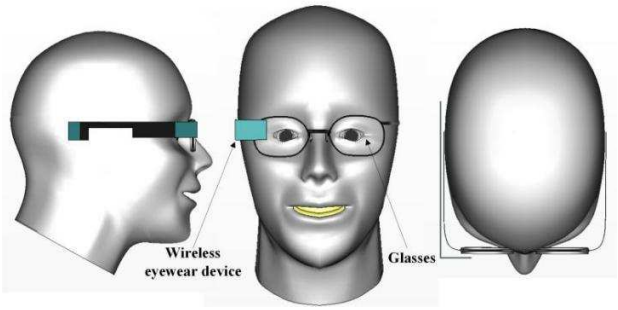

Fig. 7. Model of phone call state with glasses

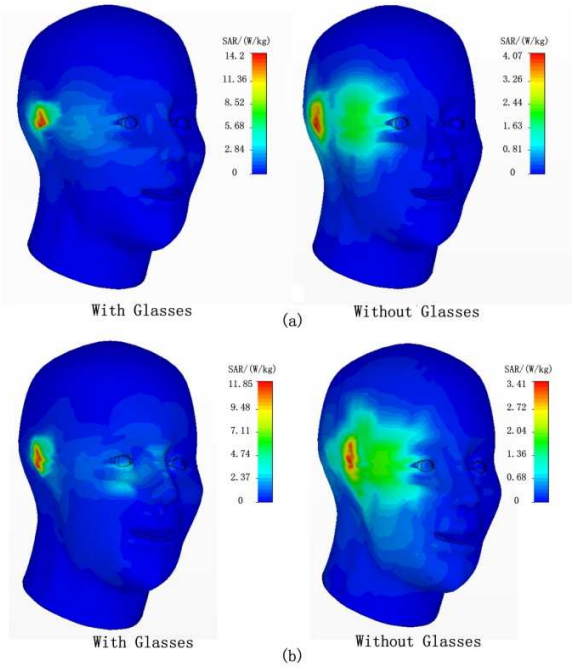

Fig. 8. Distributions of the SAR in head. (a) 0.915 GHz (b) 1.8 GHz

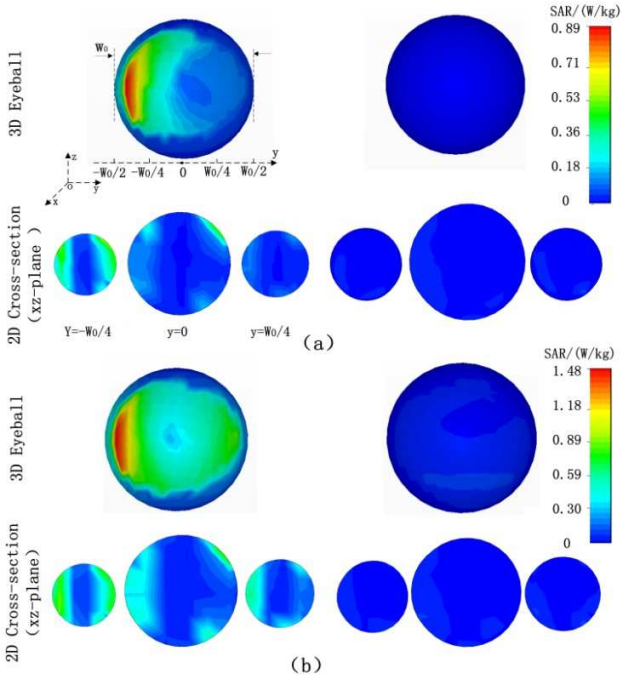

Fig. 9. Distributions of the SAR in the eyeballs at 0.915GHz. (a) Without glasses (b) With glasses

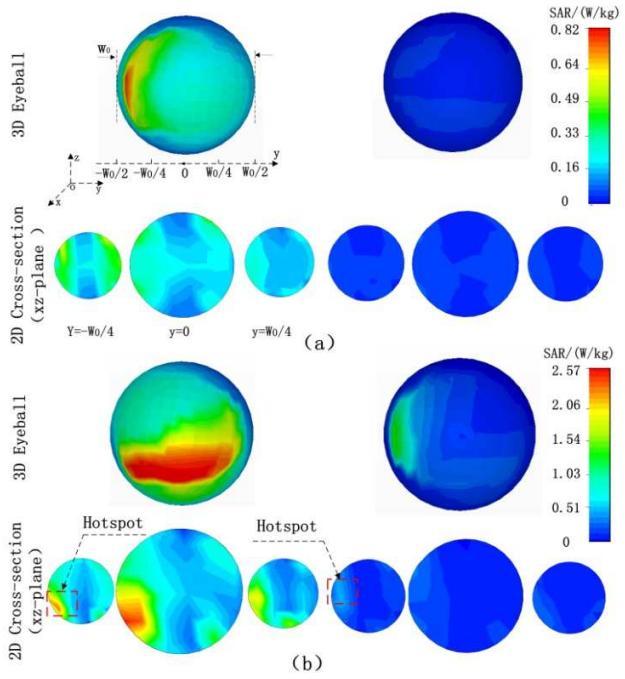

Fig. 10. Distributions of the SAR in the eyeballs at 1.8GHz. (a) Without glasses (b) With glasses

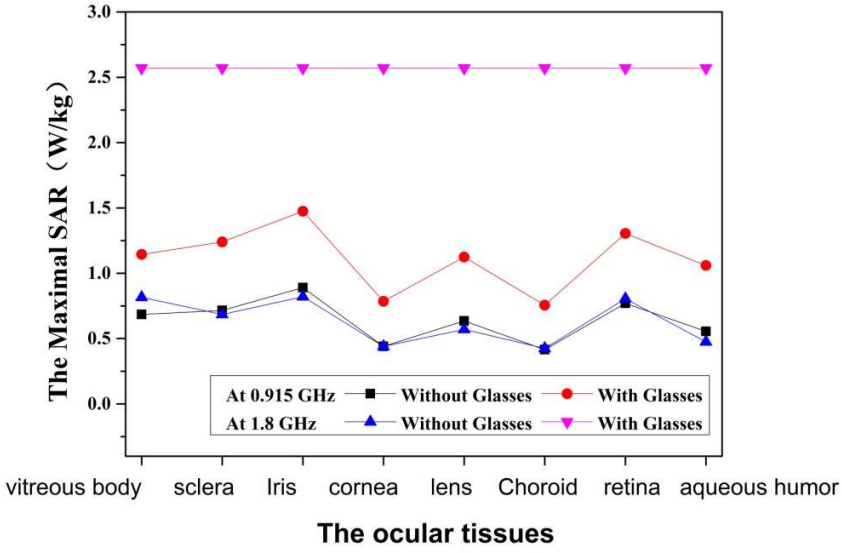

Fig. 11. The maximal SAR in ocular tissues

Secondly, we evaluate the variation of the maximal SAR in the ocular tissues with different widths of frame and thicknesses of spectacle lens. Calculated results are displayed in table 2 and table 3. We find that the maximal SAR increases with the increment of W2 and W3 at 0.915 GHz, while it decreases with the increment of W1. At 1.8GHz, The maximal SAR increases with the increment of W1. Unlike that which varies monotonically, the maximal SAR first increases and then decreases with the increment of W2. The maximal SAR shows the contrary variation trend with the increment of W3 except that in the sclera. We also find that the maximal SAR in all ocular tissues are equal in some cases at 1.8 GHz. This is due to the relative large hotspot which across all the tissues as is shown in Fig. 10. The biggest increment of SAR in the ocular tissues appears at the new hotspot. Calculated results indicate that the maximal SAR is sensitive to the frame width and radiation frequency.

Table 2

The maximal SAR in the ocular tissues at 0.915 GHz when people wear glasses with

different widths of frame and thicknesses of spectacle lens.

	W2=2mm,W3=3mm			W1=4mm,W3=3mm			W1=4mm,W2=2mm		
	W1			W2			W3		
	2mm	4mm	6mm	1mm	2mm	3mm	3mm	6mm	9mm
Vitreous Body	1.21	1.15	1.08	1.13	1.15	1.16	1.15	1.25	1.30
Aqueous humor	1.09	1.06	0.96	1.05	1.06	1.06	1.06	1.14	1.16
Sclera	1.57	1.48	1.38	1.46	1.48	1.50	1.48	1.62	1.68
Iris	0.81	0.79	0.77	0.77	0.79	0.79	0.79	0.85	0.87
Cornea	1.18	1.13	1.03	1.11	1.13	1.13	1.13	1.22	1.25
Lens	0.78	0.76	0.74	0.74	0.76	0.75	0.76	0.81	0.83
Choroid	1.38	1.31	1.22	1.29	1.31	1.32	1.31	1.43	1.47
Retina	1.31	1.24	1.17	1.23	1.24	1.26	1.24	1.36	1.40

Table 3

The maximal SAR in the ocular tissues at 1.8 GHz when people when people wear glasses with different widths of frame and thicknesses of spectacle lens.

	W2=2mm,W3=3mm			W1=4mm,W3=3mm			W1=4mm,W2=2mm		
	W1			W2			W3		
	2mm	4mm	6mm	1mm	2mm	3mm	3mm	6mm	9mm

Vitreous Body	2.63	2.57	2.49	2.56	2.57	2.36	2.57	1.28	1.81
Aqucous humor	2.63	2.57	2.49	2.56	2.57	2.36	2.57	1.76	1.77
Sclrea	2.63	2.57	2.49	2.56	2.57	2.36	2.57	2.09	2.01
Iris	2.63	2.57	2.49	2.56	2.57	2.36	2.57	1.56	1.57
Cornea	2.63	2.57	2.49	2.56	2.57	2.36	2.57	1.78	1.80
Lens	2.63	2.57	2.49	2.56	2.57	2.36	2.57	1.53	1.54
Choroid	2.63	2.57	2.49	2.56	2.57	2.36	2.57	1.81	1.87
Retina	2.63	2.57	2.49	2.56	2.57	2.36	2.57	1.79	1.84

Finally, we evaluate the effects of arm length of glasses on the SAR in the ocular tissues and show the calculation results in Fig. 12 and Fig. 13. The arm length, in the Fig. 12 and 13, changes from 80mm to 131mm with the variation interval of 3mm. We can find that the maximal SAR in the ocular tissues varies greatly with the changing length of arms. The maximal effects could be seen at 0.915GHz and 1.8GHz with the arm 131mm and 86mm, respectively. This is mainly due to the reason of resonance effect. These calculation results could provide valuable reference for the glasses designer to reduce the SAR in the eyes.

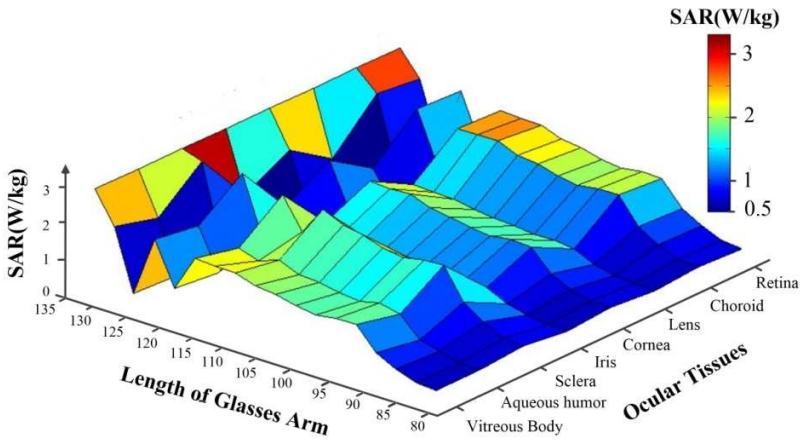

Fig. 12. The maximal SAR in the ocular tissues with different lengths of glasses arms at 0.915 GHz.

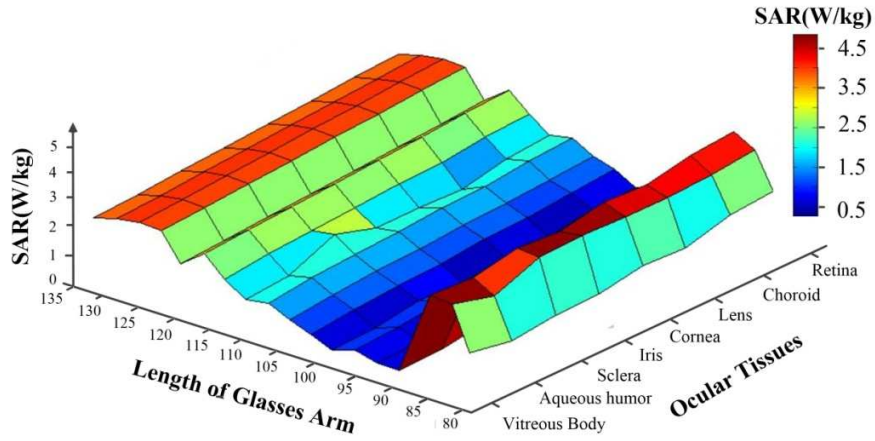

Fig. 13. The maximal SAR in the ocular tissues with different lengths of glasses arms at 1.8 GHz.

4. Conclusions

Based on the calculated results, we find wearing glasses obviously alters the distribution and magnitude of SAR. The maximal SAR in the ocular tissues with glasses is even 6 times more than that without glasses. Wearing glasses also could induce the new hotspot in the eyeballs which may cause the biggest SAR increment in the ocular tissues. Moreover, calculated results indicate that the maximal SAR is sensitive to the size of

glasses and radiation frequency. Therefore, we believe wearing glasses may possibly increase the risk of health hazard to human eyes. In order to decrease the SAR in the ocular tissues, people should choose the adaptive glasses according to the radiation frequency. These calculated results could be a valuable reference for the glasses designer to reduce the SAR in the eyes. However, due to the limited research conditions, the experiment is not included. So conclusions, in this paper, are just indicative but not definitive.

5. Acknowledgment

This project is supported by the National Science Foundation of China [Grant No.61640008].

References

International Agency for Research on Cancer, 2011. IARC classifies radiofrequency electromagnetic fields as possibly carcinogenic to humans. Press release, (208).

IEEE Std C95.1a-2010 (Amendment to IEEE Std C95.1-2005) IEEE Standard for Safety Levels with Respect to Human Exposure to Radio Frequency Electromagnetic Fields, 3kHz to 300 GHz e Amendment 1: Specifies Ceiling Limits for Induced and Contact Current, Clarifies Distinctions between Localized Exposure and Spatial Peak Power Density, 2010, pp. C1-C9.

Ahlbom, A., Bergqvist, U., Bernhardt, J. H., Cesarini, J. P., Grandolfo, M., Hietanen, M.,

McKinlay, A.F., Repacholi, M. H., Sliney, D. H., Stolwijk, J. A. J., Swicord, M. L., Szabo, L. D., Taki, M., Tenforde, T. S., Jammet, H. P., Matthes, R., 1998. Guidelines for limiting exposure to time-varying electric, magnetic, and electromagnetic fields (up to 300 GHz). Health physics, 74(4), 494-521.

Yoshida, K., Hirata, A., Kawasaki, Z., Shiozawa, T., 2005. Human head modeling for handset antenna design at 5GHz band. J. Electromagnet. Wave. 9, 401–411.

Manapati, M. B., Kshetrimayum, R. S., 2009. SAR reduction human head from mobile phone radiation using single negative meta-materials. J. Electromagnet. Wave. 23, 1385–1395.

Wake, K., Varsier, N., Watanabe, S., Taki, M., Wiart, J., Mann, S., Deltour, I., Cardis, E., 2009. The estimation of 3D SAR distributions in the human head from mobile phone compliance testing data for epidemiological studies. Phys. Med. Biol. 54, 5695–5706.

Hossain M. I., Faruque, M. R. I., Islam, M. T., 2015. Analysis on the effect of the distances and inclination angles between human head and mobile phone on SAR. Progress in biophysics and molecular biology. 119(2), 103-110.

Anzaldi, G., Silva, F., Fernandez, M., Quilez, M., Riu, P. J., 2007. Initial analysis of SAR from a cell phone inside a vehicle by numerical computation biomedical engineering. IEEE T. Bio-Med. eng. 54, 921–930.

Beard, B. B., Kainz, W., Onishi, T., Iyama, T., Watanabe, S., Fujiwara, O., Wang, J. Q., Bit-Babik, G., Faraone, A., Wiart, J., Christ, A., Kuster, N., Ae-Kyoung, L., Kroeze, H., Siegbahn, M., Keshvari, J., Abrishamkar, H., Simon, W., Manteuffel, D., Nikoloski, N., 2006. Comparisons of computed mobile phone induced SAR in the SAM phantom to that in anatomically correct models of the human head. IEEE Tronr. Eleerro. Mogn. Comp. 48, 397–407.

Chandupatla, U., Di Nallo, C., Babij, T. M., De Ponce, L., 2006. Evaluation of SAR in a homogenous head model for clam-shell type cellular phones. Antennas and Propagation Society International Symposium. IEEE, 2105-2108.

Pisa, S., Cavagnaro, M., Lopresto, V., Piuzzi, E., Lovisolo, G. A., Bernardi, P. 2005. A procedure to develop realistic numerical models of cellular phones for an accurate evaluation of SAR distribution in the human head. IEEE Trans. Microwave Theory Tech. 53, 1256 – 1265.

Schiavoni, A., Bertotto, P., Richiardi, G., Bielli, P., 2000. SAR Generated by commercial cellular phones–phone modeling, head modeling, and measurements. IEEE Trans.

Microwave Theory Tech. 48, 2064–2071.

Van Leeuwen, G. M. J., Lagendijk, J. J. W., Van Leersum, B. J. A. M., Zwamborn, A. P. M., Hornsleth, S. N., Kotte, A. N. T. J., Calculation of change in brain temperatures due to exposure to a mobile phone. Phys. Med. Biol. 44, 2367–2379.

Bernardi, P., Cavagnaro. M., Pisa, S., Piuzzi, E., SAR Distribution and temperature increase in an anatomical model of the human eye exposed to the field radiated by the user antenna in a wireless LAN. 1998. IEEE Trans. Microwave Theory Tech. 46, 2074–2082.

Scott, J. A. The computation of temperature rises in the human eye induced by infrared radiation. 1988. Phys. Med. Biol. 33, 243–257.

Cabedo, A., Anguera, J., Picher, C., Ribó, M., Puente, C., 2009. Multi-band handset antenna combininga PIFA, slots, and ground plane modes. IEEE Trans. Antennas Propag. 57, 2526–2533.

Anguera, J., Sanz, I., Mumbrú, J., Puente, C., 2010. Multi-band handset antenna with a parallel excitation of pifa and slot radiators. IEEE Trans. Antennas Propag. 58, 348–356.

Picher, C., Anguera, J., Andújar, A., Puente, C., Kahng, S., 2012. Analysis of the human head interaction in handset antennas with slotted ground planes. IEEE Antennas Propag. Mag. 54, 36–56.

Lan, J. Q., Huang K. M., 2013. Evaluation of SAR in a human head with glasses exposed to radiation of a mobile phone. Journal of Electromagnetic Waves and Applications. 27(15), 1919-1930.

Whittow, W. G., Panagamuwa, C. J., Edwards, R. M., Vardaxoglou, J. C. 2008. On the effects of straight metallic jewellery on the specific absorption rates resulting from face-illuminating radio communication devices at popular cellular frequencies. Physics in medicine and biology. 53(5), 1167.

Virtanen, H., Keshvari, J., Lappalainen, R., The effect of authentic metallic implants on

the SAR distribution of the head exposed to 900, 1800 and 2450 MHz dipole near field. 2007. Physics in Medicine and Biology, 52(5), 1221.

Cihangir, A., Luxey, C., Jacquemod, G., Pilard, R., Gianesello, F., Whittow, W. G., Panagamuwa, C. J., 2014. Investigation of the effect of metallic frames on 4G eyewear antennas. Antennas and Propagation Conference, Loughborough. IEEE, 60-63

Whittow, W. G., 2004. Specific absorption rate perturbations in the eyes and head by metallic spectacles at personal radio communication frequencies. In: *PhD thesis EEE Dept.*: University of Sheffield, UK

Cihangir, A., Whittow, W. G., Panagamuwa, C. J., Ferrero,F., Jacquemod. G., Gianesello, F., Luxey, C., 2013. Feasibility study of 4G cellular antennas for eyewear communicating devices. IEEE Antennas and Wireless Propagation Letters. 12, 1704-1707.

Brien, A. H., 2004. The myopia epidemic is there a role for corneal refractive therapy?. Eye Contact Lens. 30, 244–246.

Dimbylow, P. J., Mann, S. M., 1994. SAR calculations in an anatomically realistic model of the head for mobile communication transceivers at 900 MHz and 1.8 GHz. Phys. Med. Biol. 39, 1537–1553.

Dovrat, A., Berenson, R., Bormusov, E., Lahav, A., Lustman, T., Sharon, N., Schächter, L., 2005. Localized effects of microwave radiation on the intact eye lens in culture conditions. Bioelectromagnetics. 26(5), 398-405.

Rodrigues, A. O., Malta, L., Viana, J. J., Rodrigues, L. O. C., Ramirez, J. A., 2008. A head model for the calculation of SAR and temperature rise induced by cellular phones. IEEE T. Magn. 44, 1446–1449.

Lin, J. C., 2005. Advances in electromagnetic fields in living systems. Springer. New York.

Gandhi, O. P., Lazzi, G., Furse, C. M., 1996. Electromagnetic absorption in the human

head and neck for mobile telephones at 835 and 1900 MHz. IEEE T. Microw. Theory. 44, 1884–1897.

Jensen, M. A., Rahmat-Samii, Y., 1995. EM interaction of handset antennas and a human in personal communications. P. IEEE. 83, 7–17.

Dimbylowt, P. J., Gandhif, O. P., 1991. Finite-difference time-domain calculations of SAR in a realistic heterogeneous model of the head for plane-wave exposure from 600 MHz to 3 GHz. Phys. Med. Biol. 36, 1075–1089.

Scott, J. A., 1988. A finite element model of heat transport in the human eye. Phys. Med. Biol. 33, 227–241.

Gabriel, C., Sheppard, R. J., Grant, E. H., 1983. Dielectric properties of ocular tissues at 37 degrees C. Phys. Med. Biol. 28, 43–49.

Yee, K. S., 1966. Numerical solutions of initial boundary value problems involving Maxwell's equations in isotropic media. IEEE Trans. Antennas Propag. 14, 302–307.

Sacks, Z. S., Kinsland, D. M., Lee, J. F., 1995. A perfectly matched anisotropic absorber for use as an absorbing boundary condition. IEEE Trans. Antennas Propag. 43. 1460–1463.

Gedney, S. D., 1996. An anisotropic perfectly matched layer absorbing media for the truncation of FDTD lattices. IEEE Trans. Antennas Propag. 44, 1630–1639.

Kunz, K. S., Luebbers, R. J., 1993. The finite difference time domain method for electromagnetics. CRC press.

Kim, I. S., Hoefer, W. J. 1990. A local mesh refinement algorithm for the time domain-finite difference method using Maxwell's curl equations. IEEE Transactions on Microwave Theory and Techniques, 38, 812-815.